

Lecture Notes in Civil Engineering

Yury Vankov *Editor*

Proceedings of ICEPP 2021

Efficient Production and Processing

Contents

An Algorithm for Space-Time Accumulation of Images for Thermovision Testing of Energy Objects	1
Nikolai Andreev, Damir Galeev, and Sameh Kassem	
High-Frequency Drying Processes Simulation of Wooden Tangent Towers in a Vacuum Chamber	11
Kachanov Alexander Nikolaevich, Korenkov Dmitry Andreevich, Revkov Artem Alexandrovich, Vorkunov Oleg Vladimirovich, and Maksimov Viktor Vladimirovich	
Anti-crisis Marketing at the Enterprises of the Energy Complex in a New Reality	21
Maxim Ereemeev, Irog Kublin, Anna Shindryaeva, Shakir Yagubov, and Olga Kondrashova	
Analysis of Digital Intellectual Devices Functioning Under Electromagnetic and Electromechanical Transient Processes in Power Systems	31
Alexey V. Mokeev	
Energy Efficiency Analysis of Control Algorithms for Fan Electric Drives in Gas Air-Cooling Plants	46
Ivan Artyukhov, Alexander Abakumov, Artem Zemtsov, Yerbol Yerbayev, and Viktor Zakharov	
Improving the Environmental Performance of the Diesel Engine (21/21) by Upgrading the Fuel Supply System	56
Leonid Plotnikov, Yuri Brodov, and Nikita Grigoriev	
Calculation and Diagnostic System of the Technical Condition of Grounding Devices of Electrical Installations	64
Ivanova Viliya Ravilevna, Ivanov Igor Yurevich, and Kiselev Igor Nikolaevich	



High-Frequency Drying Processes Simulation of Wooden Tangent Towers in a Vacuum Chamber

Kachanov Alexander Nikolaevich¹(✉), Korenkov Dmitry Andreevich¹,
Revkov Artem Alexandrovich¹, Vorkunov Oleg Vladimirovich²,
and Maksimov Viktor Vladimirovich²

¹ Orel State University Named After I.S. Turgenev, Orel, Russia
kan@ostu.ru

² Kazan State Power Engineering University, Kazan, Russia

Abstract. The purpose of the work is to develop the theoretical foundations of vacuum-high-frequency drying of wooden support blanks. The use of this drying technology is currently complicated by a number of unresolved scientific and technical problems like optimizing vacuum high-frequency drying modes and ensuring electromagnetic field uniformity in long workpieces. As a result, a mathematical model was developed using the positions of the theory of electromagnetic field, heat mass transfer and heat mass exchange, methods of mathematical simulating. Also the results of previous studies of electromagnetic field distribution in the cross-section and longitudinal sections of the working chamber loading are taken into account. The obtained by using the proposed model and the method of its analysis the numerical study results are compared with the available experimental data. Based on this comparison it is concluded that the obtained model is adequate and more effective relative to other existing models of vacuum-high-frequency drying. Generally, further use of the presented mathematical toolkit to optimize the design and modes of vacuum high-frequency complexes in the task of drying wooden tangent towers will increase the reliability of overhead transmission lines.

1 Introduction

Historically, the first tangent towers of overhead power lines were wooden due to their low cost, availability and sufficient mechanical strength of the raw material. When producing power tangent towers, soft hardwood billets (birch, aspen, alder) with a length less than 8 m and conifers (pine, spruce) with a length less than 12 m [1] are used as raw materials. At the moment, wooden support is a rather complex technical product, in the process of production of which are used such steps as edging, drying, impregnation and fixing [2]. Wood modification technologies made it possible to raise the relatively low physical and mechanical properties of cheap rocks to the level of hard hardwood. The standard service life of wooden soaked tangent towers is 25 years, of reinforced concrete tangent towers is 40 years, of metal tangent towers is 50 years. Modern wood modification technologies on average make it possible to bring the service life closer to the level of reinforced concrete supports [1, 3], but not all their potential has been realized yet. Obviously,

further scientific and technical developments in this area should focus on reaching the next “psychological mark” of 50 years.

Common to all wood modification methods is a drying step in which free moisture is removed from the intercellular space. At the same time, space for modifying liquid is released. The drying quality is determined by a variety of parameters. The drying uniformity determines how uniformly the subsequent of the wood impregnation will be performed. The main type of drying defects is cracking, the more they are, and the deeper they are, the stronger the inner layers of wood will interact with negative atmospheric factors. Thus, drying is a responsible stage in the production of wooden tangent towers, which largely determines the quality of subsequent operations, and affects the standard service life of the final product.

In most cases, the tangent towers are dried by atmospheric or chamber convective methods to a moisture content of 0.28 kg/kg. The atmospheric drying disadvantage is its seasonality. Such drying is possible only in the summer and lasts about three months, but does not require additional energy consumption. The resulting cracking is considered a reference. Chamber drying allows reducing the process duration to a week and is carried out in special installations, but requires a lot of thermal energy. Another method of drying in special autoclaves under vacuum has become less common. The duration of such a method is comparable to a convective chamber, but the specific energy consumption is longer. However, there are already promising scientific and technical developments that reduce drying time at comparable or lower energy costs and are based on dielectric heating [4–6].

Nowadays combined drying technologies are becoming more and more widespread: convective-dielectric and vacuum-dielectric ones. The latter has a number of advantages. Firstly, the drying is done in a low-pressure steam-gas mixture, so a large gradient of moisture content across the section is eliminated. Secondly, due to the low boiling point of moisture, the material is heated to 80 °C, which leads to reduced heat losses through the chamber walls and the conservation of its mechanical and aesthetic properties. Thirdly, the drying speed is up to 10 times higher than the speed of the convective steam drying. The calculations show that for comparable volumes of loading of vacuum-high-frequency and convective-steam chambers, the first one helps to reduce the unit cost of lumber drying [7].

However, there are still a number of unresolved issues that limit the widespread introduction of vacuum-high-frequency technology for drying tangent towers. The existing high-frequency equipment requires a large power consumption. This leads to a decrease in competitiveness compared to convective steam chambers with a large load volume. Currently, the use of vacuum-high-frequency technology is recommended for lumber of thick sections, finewood and wood with high density. However, the drying modes of such lumber have not been fully developed yet, which requires further theoretical research in this field. This requires mathematical models that adequately describe the processes in the chamber and in the material. Development of such a mathematical apparatus is the purpose of this study, and its relevance is beyond doubt, since it is aimed at eliminating these restrictions on the use of vacuum-high-frequency drying for blanks of wooden tangent towers. Successfully overcoming the restrictions will achieve positive energy-saving and economic effects by reducing drying times and the cycle of production of

tangent towers in general. An additional beneficial effect is to provide the high drying quality required to achieve their long service life.

2 Mathematical Model

The vacuum-high-frequency chambers consist of a working chamber, usually cylindrical in shape, near which an HF generator is installed, which supplies the voltage U with a frequency f to the plates of the working capacitor via high-frequency feeders. Between the plates, on a special cart there is a material to be dried. After the generator is switched on, the internal heat sources Q_V are created in the material, and the temperature T of its internal zones increases rapidly, forming a temperature gradient directed inside the material. The moisture begins to evaporate intensively in the material, the partial pressure of steam becomes larger than the ambient pressure P_a in the chamber, which is lowered by a vacuum pump before drying. Due to the capillary-porous structure of wood near its surface, the pressure is relaxed, and a gradient of excess pressure directed to the internal zones occurs. Under the influence of temperature and pressure gradients, the thermal diffusion and filtration flows of moisture to the surface occur.

Due to evaporation, the moisture content u in the inner zones is less than in the surface ones. This creates a gradient of moisture content and a corresponding diffusive flow of moisture directed deep into the material and preventing the removal of moisture from it. The studies [8, 9] have shown that the filtration mechanism of vaporous moisture transfer to the surface becomes prevailing and explains the high intensity of high-frequency vacuum drying. The moisture transferred to the surface by the mechanisms of thermal and filtration diffusion evaporates into the surrounding space, and then condenses on the walls of the working chamber and flows into the condensate collector.

Thus, high-frequency vacuum drying is a combination of complex electrophysical, thermodynamic and heat and mass transfer processes. The complex of processes of heat and mass transfer inside the material under the influence of the considered gradients is described by the system of Lykov equations [10–15].

To simplify it, the authors used the assumption that the loss of moisture under the influence of the pressure gradient can be considered in the form [16]:

$$\frac{\partial u}{\partial \tau} = -\frac{Q_v}{r \cdot \rho_0}, \quad (1)$$

where r is the specific heat of evaporation, J/kg; ρ_0 is the density of dry material, kg/m³.

Therefore, the initial system is rearranged in the form:

$$\begin{aligned} \frac{\partial T}{\partial t} &= \frac{\partial}{\partial x} \left(a_t(T, u) \frac{\partial T}{\partial x} \right) + \frac{Q_v(x, t)}{c(T, u) \cdot \rho_0} (1 - \xi(T, u)), \\ \frac{\partial u}{\partial t} &= \frac{\partial}{\partial x} \left[a_m(T, u) \left(\delta(T, u) \frac{\partial T}{\partial x} + \frac{\partial u}{\partial x} \right) \right] - \xi(T, u) \frac{Q_v(x, t)}{\rho_0 \cdot r(T)}, \end{aligned} \quad (2)$$

where a_t is the temperature diffusivity coefficient, m²/sec; ξ is the phase transformation number; c is the specific heat of the material, J/(kg · °C); a_m is the coefficient of moisture

conductivity (diffusion of moisture), m^2/sec ; δ is the relative coefficient of thermal diffusion of moisture, $\text{kg}/(\text{kg} \cdot ^\circ\text{C})$.

Boundary conditions are used for the heat and mass transfer problem [17]:

$$\begin{aligned}\lambda_x(T, u) \frac{\partial T(L, t)}{\partial x} &= \alpha_t(T_a - T(L, t)) + r(T) \cdot j(t), \\ \rho_0 \cdot a_m(T, u) \left(\delta(T, u) \frac{\partial T}{\partial x} + \frac{\partial u}{\partial x} \right) &= j(t), \\ j(t) &= \alpha_m \rho_{\text{vap}}(T) (u_a(T_a, P_a) - u(L, t)), \\ \frac{\partial T(0, t)}{\partial x} &= 0; \quad \frac{\partial u(0, t)}{\partial x} = 0,\end{aligned}\quad (3)$$

where λ_x is the thermal conductivity along the fibers, $\text{W}/(\text{m} \cdot ^\circ\text{C})$; α_t is the coefficient of convective heat exchange, $\text{W}/(\text{m}^2 \cdot ^\circ\text{C})$; T_a is the ambient temperature, $^\circ\text{C}$; j is the surface moisture flow, $\text{kg}/(\text{m}^2 \cdot \text{sec})$, α_m is the moisture exchange coefficient, m/sec ; ρ_{vap} is the steam density, kg/m^3 ; u_a is the equilibrium moisture of the ambient.

The initial conditions reflect the uniformity of the initial temperature T_0 and moisture content u_0 according to the model.

$$T(x, 0) = T_0, \quad u(x, 0) = u_0. \quad (4)$$

The theoretical and experimental studies [18–21] show that the intensity of the processes occurring in the material is significantly affected by the uneven distribution of internal heat sources Q_v , and the maximum unevenness is observed along the material. Therefore, for an adequate description of heat and mass transfer, it is necessary to set out the distribution of internal heat sources properly, that according to the expression is:

$$Q_v(x, t) = 2\pi f \varepsilon_0 \varepsilon(T; u) \text{tg} \delta(T; u) |\dot{E}(x)|^2, \quad (5)$$

where ε , δ are the relative permittivity and the angle of dielectric losses of the material, is reduced to the problem of finding the distribution of the electric field intensity $\dot{E}(x)$. The distribution $\dot{E}(x)$ along the length of the working capacitor filled with a wood dielectric is studied in detail in [20, 21], where the following model is recommended for mathematical description of such distribution:

$$\frac{\partial^2 \dot{E}(x)}{\partial x^2} - \tilde{k}^2(x) \dot{E}(x) = 0 \quad (6)$$

$$\tilde{k}(x) = i \cdot 2\pi f \sqrt{\varepsilon_0 \mu_0 \varepsilon(T, u) (1 - i \cdot \text{tg} \delta(T, u))} \quad (7)$$

$$\frac{\partial \dot{E}(0)}{\partial x} = \tilde{k}(0) \cdot [\dot{E}(0) - E_{\text{max}}]; \quad \frac{\partial \dot{E}(L)}{\partial x} = 0, \quad (8)$$

where \tilde{k} is the wave coefficient, E_{max} is the amplitude of the electric field of the incident wave, V/m .

The joint consideration of the problems of heat and mass transfer (2)–(4) and electromagnetic one (5)–(8) allows to reflect the processes occurring inside the material

at vacuum-high-frequency drying mathematically, but for a complete description of all phenomena, it is necessary to take into account the changes in the parameters of the surrounding medium in the working chamber, since they effect the intensity of heat and moisture exchange on the surface of the material. The changes in ambient temperature and pressure are described by the equations:

$$\frac{dP_g(t)}{dt} = P_g(t) \left(\frac{1}{T_a(t)} \frac{dT_a(t)}{dt} - \frac{Q_{\text{gas}}}{V_{\text{F.V.}}} \right);$$

$$\frac{dP_{\text{vap}}(t)}{dt} = \frac{SRT_a(t)}{V_{\text{F.V.}} \mu_{\text{vap}}} j(t) - P_{\text{vap}}(t) \left[\frac{Q_{\text{vap}}}{V_{\text{F.V.}}} - \frac{1}{T_a(t)} \frac{dT_a(t)}{dt} \right]; \quad (9)$$

$$\frac{dT_a(t)}{dt} = \frac{\alpha_t S [T(L,t) - T_a(t)] RT_a(t)}{(\mu_{\text{vap}} \rho_{\text{vap}} + \mu_g \rho_g) c_a V_{\text{F.V.}}} + \frac{c_{\text{vap}} S T(L,t) j(t) RT_a(t)}{(\mu_{\text{vap}} \rho_{\text{vap}} + \mu_g \rho_g) c_a V_{\text{F.V.}}} - \frac{(Q_{\text{gas}} + Q_{\text{vap}}) T_a(t)}{V_{\text{F.V.}}},$$

$$P_a(t) = P_{\text{vap}}(t) + P_g(t), \quad T_a(0) = T_{a0}, \quad P_a(0) = P_{a0},$$

where P_{vap} , P_g are the steam and gas pressure, respectively, Pa; S is the surface area of the material, m^2 ; R is the universal gas constant; $V_{\text{F.V.}}$ is the free volume of the chamber, m^3 ; μ_{vap} , μ_g are the molar mass of steam and gas, respectively, kg/mol ; ρ_{vap} , ρ_g are the density of steam and gas, m^3/kg ; Q_{vap} , Q_{gas} are the productivity of steam and gas removal systems, m^3/sec ; c_{vap} , c_a is the heat capacity of steam and steam and gas medium, respectively, $\text{J}/(\text{kg} \cdot ^\circ\text{C})$; T_{a0} is the initial temperature of the surrounding medium, $^\circ\text{C}$; P_{a0} is the initial pressure in the chamber, taken equal to the atmospheric one, Pa.

Thus, based on the analysis of literary sources and using the results of previous studies, a mathematical apparatus is obtained that describes the influence of the wave nature of the distribution of electromagnetic field parameters along the tangent towers length and external medium parameters on the temperature and moisture content of the material. It differs from the existing mathematical models [22-25] of vacuum-high-frequency drying are the possibility of using simple methods of analyzing systems of differential equations and requiring less initial data on the properties of the dried material.

3 Materials and methods

As the presented model shows the relationship of various physical phenomena, and the properties of the material have a nonlinear character of dependence on temperature and moisture content, then only the numerical analysis can be carried out for it. The one-dimensionality of the problem allows to choose a numerical method of finite differences, for which the time step and the coordinate increment x are determined by the relations:

$$\Delta t = t_{\max} / (N_t - 1), \Delta x = L / (N_x - 1), \quad (10)$$

where N_t, N_x is the number of nodes in time and in the coordinate of the finite difference grid.

The calculation algorithm in the form of a block-scheme is shown in Fig. 1. The initial parameters are: $L, W, S, V_{F.V.}, U, f, Q_{\text{vap}}, Q_{\text{gas}}, T_0, u_0, T_{a0}, P_{a0}, \rho_0$, and the functions are: $a_t(T, u), a_m(T, u), \delta(T, u), \xi(T, u), r(T), c(T, u), \varepsilon(T, u), \text{tg}\delta(T, u)$.

At the first stage of the calculation, the distribution of internal heat sources is determined in accordance with the finite difference equations for the current time layer i given below:

$$\tilde{k}_j = i \cdot 2\pi f \sqrt{\varepsilon_0 \mu_0 \varepsilon(T_j^{i-1}, u_j^{i-1}) (1 - i \cdot \text{tg}\delta(T_j^{i-1}, u_j^{i-1}))}, \quad (11)$$

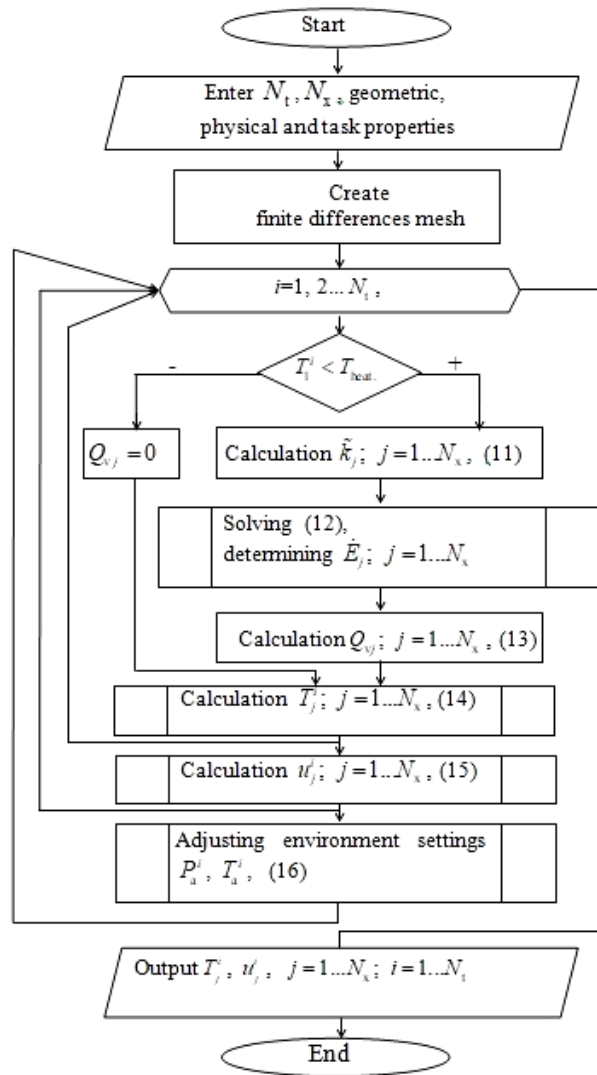


Fig. 1. Algorithm for analysing the mathematical model

$$\dot{E}_j (1 + \tilde{k}_j \Delta x) - \dot{E}_{j+1} = \tilde{k}_j \Delta x \cdot E_{\max} \quad \text{if } j = 1;$$

$$\frac{1}{\Delta x^2} \dot{E}_{j-1} - \left(\frac{2}{\Delta x^2} + \tilde{k}_j^2 \right) \dot{E}_j + \frac{1}{\Delta x^2} \dot{E}_{j+1} = 0 \quad \text{if } j = 2 \dots N_x - 1; \quad (12)$$

$$\dot{E}_j - \dot{E}_{j-1} = 0 \quad \text{if } j = N_x,$$

$$Q_{vj} = 2\pi f \varepsilon_0 \varepsilon (T_j^{i-1}; u_j^{i-1}) \text{tg} \delta (T_j^{i-1}; u_j^{i-1}) \left| \dot{E}_j \right|^2. \quad (13)$$

Then the heat and mass transfer problem is solved in two stages using an explicit scheme. At the first stage, the temperature field is calculated for the current time layer:

$$T_j^i = T_{j+1}^i \quad \text{if } j = 1;$$

$$\begin{aligned} T_j^i = T_j^{i-1} + \frac{\Delta t}{\Delta x^2} & \left[\frac{a_t(T_{j+1}^{i-1}, u_{j+1}^{i-1}) + a_t(T_{j+1}^{i-1}, u_{j+1}^{i-1})}{2} \times \right. \\ & \times (T_{j+1}^{i-1} - T_j^{i-1}) - \frac{a_t(T_j^{i-1}, u_j^{i-1}) + a_t(T_{j-1}^{i-1}, u_{j-1}^{i-1})}{2} \times \\ & \left. \times (T_j^{i-1} - T_{j-1}^{i-1}) + \frac{Q_{vj} \cdot \Delta x^2}{c(T_j^{i-1}, u_j^{i-1}) \cdot \rho_0} \right] \quad \text{if } j = 2 \dots N_x - 1; \end{aligned} \quad (14)$$

$$T_j^i = T_{j-1}^i + \frac{2\Delta x \left[\alpha_t (T_a^{i-1} - T_j^{i-1}) + r(T_j^{i-1}) \cdot j^i \right]}{\lambda_x(T_j^{i-1}, u_j^{i-1}) + \lambda_x(T_{j-1}^{i-1}, u_{j-1}^{i-1})} \quad \text{if } j = N_x; \quad j^i = \alpha_m \rho_{\text{vap}} (T_N^{i-1}) \left[u_a(T_a^{i-1}, P_a^{i-1}) - u_N^{i-1} \right].$$

At the second stage, the moisture content field is calculated:

$$u_j^i = u_{j+1}^i \quad \text{if } j = 1;$$

$$\begin{aligned} u_j^i = u_j^{i-1} + \frac{\Delta t}{\Delta x^2} & \left[\frac{a_m(T_{j+1}^i, u_{j+1}^{i-1}) + a_m(T_{j+1}^i, u_{j+1}^{i-1})}{2} \times \right. \\ & \times (u_{j+1}^{i-1} - u_j^{i-1}) - \frac{a_m(T_j^i, u_j^{i-1}) + a_m(T_{j-1}^i, u_{j-1}^{i-1})}{2} \times \\ & \times (u_j^{i-1} - u_{j-1}^{i-1}) + \frac{\psi(T_{j+1}^i, u_{j+1}^{i-1}) + \psi(T_{j+1}^i, u_{j+1}^{i-1})}{2} \times \\ & \times (T_{j+1}^i - T_j^i) - \frac{\psi(T_j^{i-1}, u_j^{i-1}) + \psi(T_{j-1}^{i-1}, u_{j-1}^{i-1})}{2} \times \\ & \left. \times (T_{j-1}^{i-1} - T_j^{i-1}) - \xi(T_j^i, u_j^{i-1}) \frac{Q_{vj} \Delta x^2}{\rho_0 \cdot r(T_j^i)} \right] \quad \text{if } j = 2 \dots N_x - 1; \\ u_j^i = u_{j-1}^{i-1} + \Delta x & \left\{ \frac{j^i}{\rho_0 \left[a_m(T_j^i, u_j^{i-1}) + a_m(T_{j-1}^i, u_{j-1}^{i-1}) \right]} - \right. \end{aligned} \quad (15)$$

$$-\frac{\delta(T_j^i, u_j^{i-1}) + \delta(T_{j-1}^i, u_{j-1}^{i-1})}{2} \frac{T_j^i - T_{j-1}^i}{\Delta x} \} \text{ if } j = N_x.$$

where $\psi(T, u) = a_m(T, u)\delta(T, u)$.

At the final stage of the calculation, the parameters of the surrounding medium are corrected:

$$\begin{aligned} T_a^i &= T_a^{i-1} + \Delta t \cdot \left\{ \frac{\left[\alpha_t S(T_{N_x}^i - T_a^{i-1}) + c_{\text{vap}} S T_{N_x}^{i-1} j^i \right] R}{(\mu_{\text{vap}} \rho_{\text{vap}} + \mu_g \rho_g) c_a V_{\text{F.V.}}} - \right. \\ &\quad \left. - \frac{Q_{\text{gas}} + Q_{\text{vap}}}{V_{\text{F.V.}}} \right\} T_a^{i-1}; \\ P_g^i &= P_g^{i-1} + \Delta t \cdot P_g^{i-1} \left(\frac{1}{T_a^i} \frac{T_a^i - T_a^{i-1}}{\Delta t} - \frac{Q_{\text{gas}}}{V_{\text{F.V.}}} \right); \\ P_{\text{vap}}^i &= P_{\text{vap}}^{i-1} + \Delta t \left[\frac{S R T_a^i}{V_{\text{F.V.}} \mu_{\text{vap}}} j^i - P_{\text{vap}}^{i-1} \left(\frac{Q_{\text{vap}}}{V_{\text{F.V.}}} - \frac{1}{T_a^i} \frac{T_a^i - T_a^{i-1}}{\Delta t} \right) \right]; \\ P_a^i &= P_g^i + P_{\text{vap}}^i. \end{aligned} \quad (16)$$

4 Results

The test for the mathematical model adequacy and the accuracy of the method of its analysis was carried out by comparing the obtained theoretical results with experimental ones. In the paper [26], a high-frequency vacuum chamber equipped with a generator with parameters: $U_{\text{max}} = 1$ kV, $f = 27$ MHz was used. The samples of coniferous wood (Japanese Cryptomeria) measuring 0.85 x 0.12 x 0.12 m were dried at a heating temperature of 60 °C and at the pressure in the chamber of 6.7 kPa. The constant heating temperature was provided by on-off control according to its value in the center of the samples. The initial moisture content was $u_0 = 0.558$ kg/kg. The initial data for the simulating were conformed to the experimental conditions [26]. The missing information was determined by the preliminary numerical experiments.

The calculation results are obtained as a data set of the values of temperature and moisture content in the nodes of the spatial grid for each time step ($T_j^i, u_j^i, j=1...N_x; i=1...N_t$). By processing the initial data set using simple algorithms, vectors of temperature values during the heating period in the center and on the surface of the material ($T_1^i, T_{N_x}^i, i=1...250$) were formed, which were then interpolated and presented as continuous functions in Fig. 2.

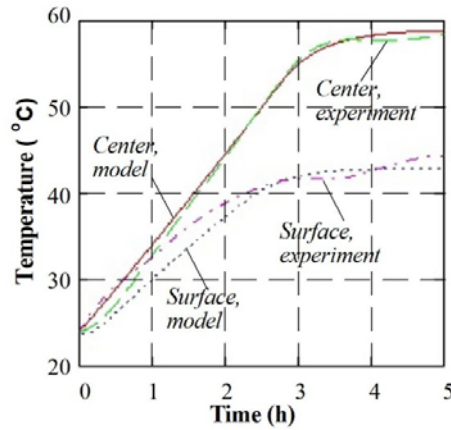


Fig. 2. Changes of the temperature in the centre and on the surface of the material at the heating stage according to the results of modelling and experiment [26]

Similarly, the graph of the dependence of the average moisture content on the drying time was obtained, Fig. 3.

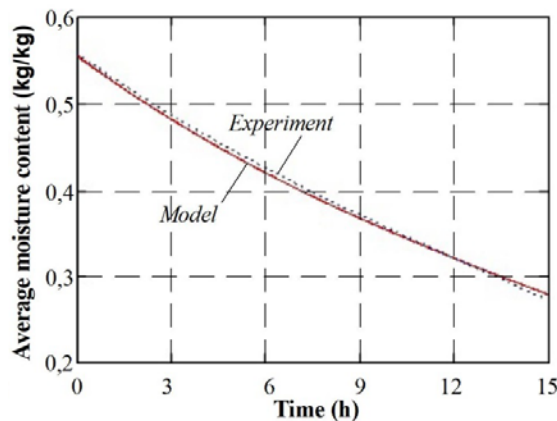


Fig. 3. Changes in the average moisture content during drying based on the results of modelling and experiment [26]

4 Discussions

The theoretical and experimental curves describing the heating in the center of the material (Fig. 2) practically match, which indicates a fairly accurate simulating of the process in the inner zones. The phenomena that occur in the surface zones are more diverse and require precise boundary conditions, which is not always possible for the reasons described. For example, in this paper, the convective heat transfer coefficient was set out constant, but in reality it depends on many factors: the method of surface processing, the temperature and moisture content of wood, as well as on the parameters of the surrounding medium. Despite this, after heating is over, both the model and the experiment show the same surface temperature of 42 °C.

The curves of changes in the average moisture content during drying (Fig. 3) also match. The absolute error does not exceed 0.006 kg / kg, which is 1.07 % of the initial moisture content. The maximum divergence of the curves is observed in the zone of transition from the drying mode at a constant speed to the drying mode at a

decreasing speed. This can be explained by the influence of the phase transformation criterion $\xi(T, u)$ set out by the chain function.

The additional numerical experiments that were carried out without taking into account the electromagnetic field distribution, showed a significant difference between the theoretical and experimental curves both for temperature and for average moisture content. The differences consisted in a 1.5-fold increase of the heating and drying speed, which contradicts the experimental data.

5 Conclusions

The used assumption (1) made it possible to simplify the initial model of heat and mass transfer and refuse to consider the mutual influence of its three driving factors. At the same time, a one-dimensional setting of the problem, taking into account the distribution of internal heat sources, turned out to be suitable for objects of long length. As a result, the amount of input data required was reduced, which ambiguously affected the applicability of the model. On the one hand, due to its ease of implementation and sufficient adequacy, it should be considered an effective means of further research in the field of working chambers design optimization (in terms of drying uniformity of wooden tangent towers and other long lumber). On the other hand, the obtained one-dimensional mathematical apparatus does not allow to study the difference in moisture content along the cross section of the material. Thus, it is not applicable to problems of optimizing drying modes, which can be solved on the basis of already existing models.

References

1. Gatiyatov I.Z., Sabitov L.S. Power engineering: research, equipment, technology **20**, 96 (2018)
2. I.N. Medvedev Forestry Bulletin **22(6)**, 103 (2018).
3. N.V. Savina, A.O. Varygina Compendium of the conference "Energy: Management, Quality and Resource Efficiency", 350 (2019)
4. V.A. Shamaev, I.N. Medvedev Collection of materials of the conference Topical directions of scientific research of the XXI century: theory and practice **2(2-1)**, 192 (2004)
5. V.P. Galkin, G.N. Kuryshov, A.A. Kosarin, S.A. Moiseev, D.I. Forestry Bulletin **2**, 62 (2018).
6. A.W. Mohd-Jamil, A.R. Zairul GCEC 2017 **9**, 191 (2017)
7. X. Zhao, C. Lee Holzforschung **75(1)**, 52, (2020)
8. A.N. Kachanov, D.A. Korenkov XI International Scientific and Practical Internet Conference "Energy and Resource Saving - XXI Century, 211 (2013)
9. D.A. Boldor, T.H. Sanders, K.R. Swartzel, B.E. Farkas J. of Food Process Engineering **28**, 68 (2005)

10. A.B. Markov, Yu.P. Yulenets Theoretical basics of chemical technology, **36(3)**, 272 (2002)
11. V.V. Komarov Wave process physics and radio engineering systems, **13(4)**, 58 (2010)
12. R. Younsi, S. Kadem, A. Lachemet, D. Kocaeffe Thermal Science, **19(2)**, 695 (2015)
13. Zhao, J.-Y., Cai, Y.-C., Fu, Z.-Y. Beijing Linye Daxue Xuebao/Journal of Beijing Forestry University **37(7)**, 123 (2015)
14. Kumar, C., Millar, G.J., Karim, M.A. Drying Tech. **33(2)**, 227 (2015)
15. M.A. Goreshnev, A.N. Kazarin, M.V. Alekseev Collection of works of the XVI International Scientific and Practical Conference of Students, Graduate Students and Young Scientists **3**, 172 (2010)
16. Sinyutin E.V., Yulenets Yu.P. Instruments and systems. Control, control, diagnostics **8**, 6 (2008)
17. Chai, H., Xu, C., Li, J., Kong, F., Cai, Y. BioResources **14(4)**, 9601 (2019)
18. Chai Hao-jie, Zhao Jing-Yao, Cai Ying-Chun. Wood and Fiber Science, **50(3)**, 340 (2018)
19. Kachanov A.N., Korenkov D.A. ICIEAM (2017).
20. A.N. Kachanov, D.A. Korenkov The Bulletin of KrasGAU **10(121)**, 142 (2016)
21. Kachanov A.N., Korenkov D.A. Industrial energy **9**, 26 (2016)
22. X. Jia, BioResources **10(3)**, 5440 (2015)
23. A. Koumoutsakos, S. Avramidis, S. Hatzikiriakos Drying Tech. **19(1)**, 65 (2001)
24. Kim, H., Han, Y., Park, Y., Lee, H.-M., Yeo, H. Journal of the Korean Wood Science and Technology **45(6)**, 769 (2017)
25. Li, X.-J., Zhang, B.-G., Li, W.-J. Drying Tech. **26(11)**, 1385 (2008)
26. H.H. Liu, L. Yang, Y. Cai, K. Hayashi, K. Li BioResources **9(2)**, 3070 (2014)